D-Optimal Design Applied to Calibration of Strapdown Three-axis Magnetometer

Zhitian Wu, Xiaoping Hu, Meiping Wu, Peng Liu
Department of Automatic Control, National University of Defense Technology
Changsha, Hunan, 410073, China
magwuzhitian@gmail.com, xiaopinghu313@163.com, meipingwu@263.net, pengliu@163.com

***Abstract*—Strapdown three-axis magnetometer needs calibration before it can be properly employed for navigation purposes. Many scalar calibration methods have been proposed to determine the calibration parameters. However, most calibration approaches seldom describe the influence of sampling distributions on the parameters estimation. As a result, some approaches lack robustness when measurement points are not well distributed. This paper presents the usage of D-optimal design to improve the accuracy and robustness of the solutions for magnetometer calibration problem. The basic idea is to choose the measurement point positions to build a D-optimal design, and then seek optimal solutions of the cost function of the D-optimal design problem by using the particle swarm optimization (PSO) algorithm. Numerical results which show the large improvement in the accuracy and robustness of the solutions are achieved.**

Keywords-Three-axis magnetometer; Scalar calibration; D-optimal design; Parameter estimation

I. INTRODUCTION *(HEADING 1)*

Strapdown three-axis magnetometer is a low cost sensor for navigation purposes. It is widely integrated by other sensors to determine the attitude or position of a vehicle [1]. The magnetometer outputs are often distorted by combined errors which result from sensor manufacturing and vehicle disturbance, and thus a calibration must be performed prior to its use.

A kind of calibration methods called scalar calibration is often used. Scalar methods convert the calibration problem into an error model parameter estimation problem, and estimate the parameter using data sets obtained from vehicle's maneuver. Since the quality of data sets may dramatically influence the accuracy and robust of parameter estimation [2], a major question we face is how to best collect measurements to enable the calibration method to efficiently and accurately estimate model parameters. This is the well-known optimal design problem [3]. An optimal design of maneuver should be carefully considered before the procedure of magnetometer calibration.

An optimal attitude motion of sensor or vehicle can provide meaningful magnetic measurements to improve a robust calibration. Unfortunately, methods on attitude motion optimization for magnetometer calibration are few. Merayo [2] considered the distribution of measurements as one of the two main sources to affect the parameters, and suggested that measurements should be distributed uniformly in all directions in vehicle's allowable attitude space. Merayo's strategy (the uniformity design method) is easy to be implemented but only suited to the case that the attitude space is regular in shape. Gebre-Egziabher [4] pointed out that a data collection scheme must be performed to reduce the effect of measurement locus, but did not describe the scheme in detail. Bonnet [5] took three data sets obtained from different movements (free rotations, rotations around East-West axis, and six static orientations) for simulated calibration comparison. Based on the simulation results, he concluded that some calibration methods are lack of robustness when measurement points are not well distributed. In a word, there are seldom criteria or principles to design a good scheme of attitude motion to obtain high quality of measurements for magnetometer calibration.

This paper presents a novel algorithm using D-optimal design which gives an optimal scheme of attitude motion for robust magnetometer calibration. The D-optimal design is a popular method for solving the optimal design problem since it has several advantages. For example, it can be applied to select a design when the experimental region is not regular in shape [6]. This property is useful for the strapdown three-axis magnetometer calibration problem.

The D-optimal design method is assessed in numerical results. The results show that data sets obtained from the proposed attitude motion by the D-optimal design greatly improves the accuracy of parameter estimates as compared with the Merayo's strategy, namely, uniform design.

Section II describes the formulation of the magnetometer calibration problem, as well as some existing calibration methods. Section III presents the D-optimal design and its application to the calibration problem. Section IV describes the seeking of optimal solutions of the D-optimal design. Numerical test is presented in Section V. Finally, the conclusion is given in Section VI.

II. MAGNETOMETER CALIBRATION

A. Backgrounds

The coordinate frames used in this paper are defined as follows.

n-frame: Orthogonal reference frame aligned with north-up-east (NUE) geodetic axes.

b-frame: Orthogonal reference frame fixed and aligned with nose-up-right of the vehicle.

s-frame: Sensor frame fixed on the magnetometer, built up from sensor's three axes.

Note that the s-frame is different from the b-frame. It is non-orthogonal with scale factor errors and offsets because the frame is affected by both sensor errors and external

Published by Atlantis Press, Paris, France.

magnetic field. If we ignore all errors, the s-frame will be identical to the b-frame.

We assume that the geomagnetic field in calibration area is homogeneous, and the reference geomagnetic vector in n-frame, denoted by $\mathbf{B}^n = \left(x^n, y^n, z^n\right)^T$, can be modeled with reasonable accuracy from the Word Magnetic Model (WMM) [7]. Its projections in b-frame are

$$\mathbf{B}^b_{\mathbf{m},t} = C^b_n(t)\mathbf{B}^n \tag{1}$$

where $t = 1, 2, ..., m$ denotes the index of the directions, $\mathbf{B}^b_{\mathbf{m},t}$ is the projections in b-frame and $C^b_n(t)$ denotes the direction cosine matrix in t step that transforms the magnetic field vector $\mathbf{B}^n$ in n-frame to the vector $\mathbf{B}^b_{\mathbf{m},t}$ in b-frame. The transformation is described by a "yaw-pitch-roll" rotation, that is

$$\begin{aligned} C^b_n(t) = &\begin{bmatrix} 1 & 0 & 0 \\ 0 & \cos(\mathrm{r}_t) & \sin(\mathrm{r}_t) \\ 0 & -\sin(\mathrm{r}_t) & \cos(\mathrm{r}_t) \end{bmatrix} \times \\ &\begin{bmatrix} \cos(\mathrm{p}_t) & \sin(\mathrm{p}_t) & 0 \\ -\sin(\mathrm{p}_t) & \cos(\mathrm{p}_t) & 0 \\ 0 & 0 & 1 \end{bmatrix} \begin{bmatrix} \cos(\mathrm{y}_t) & 0 & -\sin(\mathrm{y}_t) \\ 0 & 1 & 0 \\ \sin(\mathrm{y}_t) & 0 & \cos(\mathrm{y}_t) \end{bmatrix} \\ &\equiv T\left(Euler(t)\right) \end{aligned} \tag{2}$$

where $Euler(t) = (\mathrm{r}_t, \mathrm{y}_t, \mathrm{p}_t)$ denotes the Euler angles in t step. In actual practice, except some vehicles with low size, most vehicles cannot maneuver in the entire Euler angle space. So the Euler angles space is usually constrained as follows.

$$\Omega_{Euler} = \left\{ \begin{matrix} \min_{\mathrm{r}} < \mathrm{r} < \max_{\mathrm{r}}, \\ \min_{\mathrm{y}} < \mathrm{y} < \max_{\mathrm{y}}, \\ \min_{\mathrm{p}} < \mathrm{p} < \max_{\mathrm{p}} \end{matrix} \right\} \tag{3}$$

where Ω_{Euler} denotes Euler angles space that the vehicle can span, $\min_{\vartheta}$ and $\max_{\vartheta}$ $(\vartheta = \mathrm{r,y,p})$ denote the maximum and minimum of ϑ, respectively. Thus we have

$$Euler(t) \in \Omega_{Euler} \quad \forall t = 1, 2, ..., m \tag{4}$$

B. Magnetometer Errro Model

In general, magnetometer measurement errors result from sensor manufacturing (non-orthogonality, scale factors, and offsets) and vehicle disturbance (hard iron and soft iron errors). Mathematically, these errors are modeled as total non-orthogonality, total scale factor and total bias, which are the main results calibrated by most calibration methods [5, 8]. A unified mathematical model is used as follows:

$$\mathbf{B}^s_{\mathbf{m}} = \mathbf{C_S}\mathbf{C_N}\mathbf{B}^b_{\mathbf{m}} + \mathbf{O} + \mathbf{n} = \mathbf{K}\mathbf{B}^b_{\mathbf{m}} + \mathbf{O} + \mathbf{n} \tag{5}$$

where $\mathbf{B}^s_{\mathbf{m}}$ is the magnetometer measurement in sensor frame (s-frame). The superscript **s** indicates s-frame. $\mathbf{B}^b_{\mathbf{m}}$ is the reading in b-frame. $\mathbf{C_N}$ denotes the total non-orthogonality matrix. $\mathbf{C_S}$ is total scale factor matrix. $\mathbf{O}$ is total bias vector. $\mathbf{K} = \mathbf{C_S}\mathbf{C_N}$ is an upper triangular matrix under the assumption that the z-axis of s-frame coincides with the z-axis of b-frame [5]. $\mathbf{n}$ is measurement noise vector, which is generally assumed to be white and Gaussian and is denoted as $\mathbf{n} \sim N\left(0, \sigma^2 I_3\right)$.

A calibration model is constructed by inversing (5), that is

$$\hat{\mathbf{B}}^b_{\mathbf{m}} = \mathbf{K}^{-1}\left(\mathbf{B}^s_{\mathbf{m}} - \mathbf{O} - \mathbf{n}\right) = \mathbf{P}\left(\mathbf{B}^s_{\mathbf{m}} - \mathbf{O} - \mathbf{n}\right) \tag{6}$$

where $\hat{\mathbf{B}}^b_{\mathbf{m}}$ denotes the calibrated measurement in b-frame. The parameterized matrix $\mathbf{P} = \mathbf{K}^{-1}$ is also an upper triangle matrix.

The scalar calibration methods follow the fact that the plot of a strapdown three-axis magnetometer output with error free lies on a sphere with radius equal to the magnitude of local geomagnetic field. Thus the scalar equation is

$$R^2 = \left\|\hat{\mathbf{B}}^b_{\mathbf{m}}\right\|^2 = \mathbf{B}^{s\,T}_{\mathbf{m}}\mathbf{G}\mathbf{B}^s_{\mathbf{m}} - 2\mathbf{O}^T\mathbf{G}\mathbf{B}^s_{\mathbf{m}} + \mathbf{O}^T\mathbf{G}\mathbf{O} + \tilde{n} \tag{7}$$

where R is the total magnitude of reference magnetic field. The superscript T denotes matrix transpose operation. $\mathbf{G} = \mathbf{P}^T\mathbf{P}$ is a positive symmetrical matrix, and the scalar noise item is $\tilde{n} = -2\left(\mathbf{B}^s_{\mathbf{m}} - \mathbf{O}\right)^T\mathbf{G}\mathbf{n} + \mathbf{n}^T\mathbf{G}\mathbf{n}$. In general, we assume the original measurement noise $\mathbf{n}$ is small enough that $\tilde{n}$ is approximately white Gaussian distributed.

Expanding the scalar equation (7) gives

$$\begin{aligned} &a_1\left(B^s_x\right)^2 + a_2B^s_xB^s_y + a_3B^s_xB^s_y + a_4\left(B^s_y\right)^2 + a_5B^s_yB^s_z \\ &+a_6\left(B^s_z\right)^2 + a_7B^s_x + a_8B^s_y + a_9B^s_z + a_{10} + \tilde{n} = 0 \end{aligned} \tag{8}$$

where B^s_x, B^s_y and B^s_z are components of $\mathbf{B}^s_{\mathbf{m}}$. $a_i, i = 1, 2, ..., 10$ are defined by the calibration parameters $\mathbf{P}$ and $\mathbf{O}$.

By introducing an intermediate variable, the nonlinear scalar equations (8) can be transformed into a linear equation as follows

$$\chi = h\theta + \tilde{n} \tag{9}$$

with

$$\chi = 1$$

$$h = \left(\left(B^s_x\right)^2, B^s_xB^s_y, B^s_xB^s_z, \left(B^s_y\right)^2, B^s_yB^s_z, \left(B^s_z\right)^2, B^s_x, B^s_y, B^s_z\right)$$

$$\theta = -\frac{1}{a_{10}}\left(a_1, a_2, a_3, a_4, a_5, a_6, a_7, a_8, a_9\right)^T$$

Consider m measurements, the linear equation of each data point can be combined into a large matrix equation as

$$\mathbf{W} = \mathbf{H}\theta + \tilde{\mathbf{n}} \tag{10}$$

where $W = (1, 1, ..., 1)^T$, $\mathbf{H} = \left(h_1, h_2, ..., h_m\right)^T$, h_i is constructed by the i-th sample of $\mathbf{B}^s_{\mathbf{m}}$.

Once θ is estimated, the calibration parameters $\mathbf{P}$ and $\mathbf{O}$ can be abstracted from θ.

III. D-OPTIMAL DESIGN

A. Theoretical Results

The D-optimal design is a typical optimal experimental design method, which is designed to select optimal sampling distributions by minimizing a specific cost function for parameter estimation problems [9]. There are several optimality criteria proposed to get an optimal design, for example, A-optimal design, D-optimal design, E-optimal design and SE-optimal design [3]. Among them, the D-optimal is the most popular one.

We describe the D-optimal design from a linear regression model like (9). In this model, θ is the variable to be estimated, denoted by $\hat{\theta}$. The value of $\hat{\theta}$ can be estimated by a standard least square estimator as follows

$$\hat{\theta} = \left(H^T H\right)^{-1} H^T W \tag{11}$$

The matrix

$$M_F = H^T H \tag{12}$$

is called the information matrix.

The variance-covariance matrix of $\hat{\theta}$ is

$$V\left(\hat{\theta}\right) = \sigma^2 \left(H^T H\right)^{-1} \tag{13}$$

where σ^2 denotes the variance of the measurement errors. It is shown that the variance of $\hat{\theta}$ is influenced by the value of the information matrix.

The D-optimal design is obtained by maximizing the determinant of the information matrix M_F. That is

$$J_D\left(M_F\right) = \max \det\left(M_F\right) \tag{14}$$

$J_D\left(M_F\right)$ is the cost function of the D-optimal design. It is a continuous operation on matrices so that J_D is continuous in M_F. The higher is the determinant of the M_F, the closer to orthogonality is the M_F [6]. This is useful to the model parameters estimation because the orthogonality ensures the mutual independence of the model coefficients. Furthermore, the ill-posed problem of the system can be alleviated, thus a robust estimates may be achieved.

B. Computations

The popular algorithms for the D-optimal design are the Fddorov's or Fedorov-like algorithms [9], which are also called exchange algorithms. The basic concept of these algorithms is to iteratively replace an old candidate with minimal information of the design by a new candidate with maximal information of the design. When the number of candidates is high, these algorithms are inefficient. In our case, there are infinite candidates due to the continuous Euler angles space, so the above methods become impractical. A projected conjugate gradient algorithm was proposed in [10] to solve the D-optimal design. This method is useful in low dimensional problem but not feasible for our case, because the dimension of solutions composed by m data points is as high as $3m$. A third kind of methods are based on stochastic search algorithms. These methods are applicable to solve complex, continuous and high-dimensional problems [11].

The PSO algorithm is a stochastic search algorithm proposed by J.Kennedy and R.Eberhart [12]. This algorithm searches for an optimal point in the solution space of the optimization problem directly, and thus it is more straightforward to use in relation to the GA algorithm. Furthermore, the PSO algorithm updates its particles (solutions) both by position information and velocity information. Therefore, it generally has a faster convergent rate than other evolution algorithms. In this work, we use the PSO algorithm to solve the D-optimal design cost function.

In order to seek a practical solution of the D-optimal design minimum problem by the PSO algorithm, the cost function of the problem should be transformed into a minimization form:

$$\arg\min g\left(X\right) = \log\left(\frac{1}{\det\left(M_F\right)}\right) \tag{15}$$

A particle is defined as:

$$\begin{aligned} X &= \left[Euler(1) \quad Euler(2) \quad \ldots \quad Euler(m)\right]^T \\ &= \left[\mathrm{r}_1, \mathrm{y}_1, \mathrm{p}_1 \quad , \mathrm{r}_2, \mathrm{y}_2, \mathrm{p}_2 \quad \ldots \quad , \mathrm{r}_m, \mathrm{y}_m, \mathrm{p}_m\right]^T \\ &\equiv \left[x_1, x_2, \ldots, x_{3m}\right]^T \end{aligned} \tag{16}$$

Note that the dimension of X is $3m$.

At the k step, the position vector of the i-th particle can be presented as

$$X_i(k) = \left[x_{i-1}(k), x_{i-2}(k), \ldots, x_{i-3m}(k)\right]^T$$

The velocity vector as

$$V_i(k) = \left[v_{i-1}(k), v_{i-2}(k), \ldots, v_{i-3m}(k)\right]^T$$

The Pbest vector of this particle found so far as

$$P_i(k) = \left[p_{i-1}(k), p_{i-2}(k), \ldots, p_{i-3m}(k)\right]^T$$

The Gbest vector of the swarm found so far as

$$G_i(k) = \left[g_{i-1}(k), g_{i-2}(k), \ldots, g_{i-3m}(k)\right]^T$$

All particles adjust their velocities and positions as follows.

$$\begin{aligned} v_{i-j}(k+1) = {} & w v_{i-j}(k) + c_1 r_1 \left(p_{i-j}(k) - x_{i-j}(k)\right) \\ & + c_2 r_2 \left(g_{i-j}(k) - x_{i-j}(k)\right) \end{aligned} \tag{17}$$

$$x_{i-j}(k+1) = x_{i-j}(k) + v_{i-j}(k+1) \tag{18}$$

where i $(i = 1, 2, 3, \ldots, m)$ is the i-th particle of the swarm, j $(j = 1, 2, \ldots, 3m)$ is the j-th dimension of particle. w is an inertia weight controlling the influence of previous velocity of a particle. c_1 and c_2 are study factors, respectively. r_1 and r_2 are random scalars in the range (0,1) and keep the diversities in the swarm. In addition, the particle velocity in each dimension is limited to an interval $[-V_{\max}, V_{\max}]$. The interval controls a maximum step size the particle can move, which prevents the positions of the particles from increasing rapidly in each step [13].

The inertia weight w has provided improved performance in many applications. A suitable selection of w

provides a balance between global and local exploration and exploitation [13]. The most common strategy of selecting w is decreased linearly as

$$w = w_{\max} - \frac{w_{\max} - w_{\min}}{iter_{\max}} \times iter \tag{19}$$

where $w_{\max}$ and $w_{\min}$ denote higher and lower values of w, respectively. $iter_{\max}$ denotes the maximum number of iteration and $iter$ is the current iteration.

Procedure of the PSO-based algorithm for the problem in is summarized as follows

Initialize all particles of the PSO with random velocities and positions. Set the current positions as initial Pbest for all particles. Set the current iteration $k = 0$. Calculate the value of cost function (15) for each particle, and then select the best position as initial Gbest.

Update the velocity and position for each particle according to (17) and (18). Limit each dimension of velocity within $[-V_{\max}, V_{\max}]$ and the position within the search space.

Calculate the new fitness value of all the particles. For each particle, if the new fitness value is smaller than the fitness value of its Pbest, then replace Pbest by current position, otherwise, hold the Pbest.

Compare the fitness value of each particle and select the minimum. If this minimum is smaller than the fitness value of Gbest, replace Gbest by the particle's position which holds the minimum fitness value.

Increase the iteration $k = k + 1$. If the fitness value of the Gbest is less than a set threshold or $k = iter_{\max}$, terminate the iteration and output the Gbest; otherwise, go to 3).

Given $\mathbf{X}^*$ is the global optimum by the algorithm, the solutions of the optimization in (15) can be easily abstracted from $\mathbf{X}^*$. That is

$$Euler^*(t) = X^*(3t-2, 3t-1, 3t)^T \quad \forall t = 1, 2, ..., m \tag{20}$$

IV. SIMULATIONS

A. Experimental Setup Description

Assume that the calibration position is in Changsha city, Hunan province, China. Its reference geomagnetic vector can be modeled from the Word Magnetic Model. The reference parameters of total non-orthogonality angles $\boldsymbol{\psi}$, total scale factor $\mathbf{S}$, and total bias $\mathbf{O}$ are

$$\boldsymbol{\psi} = \begin{bmatrix} 1.5 \\ 0.8 \\ 1.4 \end{bmatrix} \text{deg}, \quad \mathbf{S} = \begin{bmatrix} 1.3 \\ 0.7 \\ 1.2 \end{bmatrix}, \quad \mathbf{O} = \begin{bmatrix} 3000 \\ -6000 \\ 5000 \end{bmatrix} \text{nT}$$

We assume that the three-axis magnetometer is strapped to an Autonomous Underwater Vehicle (AUV). The constrained maneuverability of the AUV is

$$\Omega_{Euler} = \begin{Bmatrix} -5^\circ < \mathrm{r} < 5^\circ \\ -180^\circ < \mathrm{y} < 180^\circ \\ -20^\circ < \mathrm{p} < 20^\circ \end{Bmatrix}$$

The values of parameters in the PSO are reported in Tab. 1. Our setting uses the guidelines given in [14].

Note that the search space of the particle X is composed by Ω_{Euler}, and the dynamic range of each dimension in a particle should be limited to the corresponding interval. Also the $V_{\max}$ for each dimension is set to 15% of the corresponding new dynamic range.

TABLE I. PARAMETERS VALUES

Parameters	Values	Parameters	Values
$w_{\max}$	0.9	c_1	1.8
$w_{\min}$	0.4	c_2	1.8
M	300	$iter_{\max}$	3000

B. The estimation criteria

To evaluate the accuracy of parameters estimation, three criteria are defined as:

$$\eta_\psi = \frac{\|\hat{\boldsymbol{\psi}} - \boldsymbol{\psi}\|}{\|\boldsymbol{\psi}\|} \times 100\% \tag{21}$$

$$\eta_S = \frac{\|\hat{\mathbf{S}} - \mathbf{S}\|}{\|\mathbf{S}\|} \times 100\% \tag{22}$$

$$\eta_O = \frac{\|\hat{\mathbf{O}} - \mathbf{O}\|}{\|\mathbf{O}\|} \times 100\% \tag{23}$$

where $\hat{\boldsymbol{\psi}}, \hat{\mathbf{S}}, \hat{\mathbf{O}}$ are estimates of $\boldsymbol{\psi}, \mathbf{S}, \mathbf{O}$, respectively. The superscript $\hat{}$ denotes an estimated quantity. η_ψ, η_S and η_O denote the relative error of total non-orthogonality, total scale factor and total bias, respectively. Lower value they achieve, more accuracy the estimates are.

C. Results

We choose to take as many measurement points as unknown variable in order to minimize the number of measurements. In this case, there are 9 measurement points should be chose in an allowable Euler space. The attitude motion resulted from the Uniformity design method (Merayo's method in [2]) and the D-optimal design method are listed in Tab. 2.

The D-optimal design is distributed more dispersive than the Uniformity design. Thus a better estimation of the model parameters is likely to get [10]. On the other hand, the Uniformity design cannot keep the measurement point positions distributed evenly over the allowable region due to an affine transformation in equation (5) which transforms a regular region to a non-regular one, whereas the D-optimal design is insensitive to this transformation.

We calibrate the measurement error model parameters by using the Two-Step calibration method proposed in [4]. This method is easy to be implemented. In addition, a condition number of the measurement error model can be computed

from the measurements. It is used to expose an effect of the D-optimal design on the parameter estimation.

One thousand computer runs are carried out to produce measurements from the positions in Tab. 2. These measurements are added by random noise with a standard variance $\sigma = 30\text{nT}$. The average performance of the three criteria $\eta_\psi, \eta_S, \eta_O$ for these random runs are shown in Fig. 1- Fig. 3, respectively. These figures show that all criteria of the D-optimal design are superior to that of the Unifomity design in both the mean and the standard variance aspects. The mean of the relative errors $\eta_\psi, \eta_S, \eta_O$ obtained by the D-optimal design are 9.8%, 0.5%, and 5.5%, compared with 25.5%, 0.6%, and 7.5% by the Unifomity design. Correspondingly, the standard variance are 4.5%, 0.42%, and 3.5%, compared with 16.5%, 0.45%, and 3.8%. As mentioned above, the D-optimal design considers the mutual independence of column coefficients, and hence improves the accuracy and robustness for the parameter estimates.

The ratio computations of the determinant of the information matrix M_F and the condition number of the measurement error model are reported in Tab. 3. In this table, the $M_F(*)$ and $Cond(*)$ denote the information matrix and the condition number of the two designs. D_{design} and U_{design} denote the D-optimal design and the Unifomity design, respectively. The table shows that both the determinant of the M_F^{-1} and the condition number following the D-optimal design are smaller than that of the Uniformity design. As a result, the calibration problem is more stable with the D-optimal design.

TABLE II. ATTITUDE MOTION RESULTS FROM DIFFERENT OPTIMAL DESIGN METHOS $[roll \quad yaw \quad pitch]$ (deg)

Number	Uniformity design	D-Optimal design
1	[-5.0 -60.0 -20.0]	[–5.0 -37.0 -20.0]
2	[-5.0 60.0 -20.0]	[-5.0 -145.0 -20.0]
3	[-5.0 180.0 -20.0]	[–5.0 -10.0 -6.0]
4	[0.0 -90.0 0.0]	[0.0 24.5 20.0]
5	[0.0 0.0 0.0]	[–3.2 -96.0 7.0]
6	[0.0 90.0 0.0]	[–1.3 178.0 –20.0]
7	[0.0 180.0 0.0]	[-1.4 180.0 -20.0]
8	[5.0 -60.0 20.0]	[2.1 -35.0 20.0]
9	[5.0 60.0 20.0]	[-5.0 -137.5 20.0]

TABLE III. THE RATIO OF THE DETERMINANT AND CONDITION NUMBER

Items	Value
$\lvert M_F(D_{design})\rvert^{-1} \big/ \lvert M_F(U_{design})\rvert^{-1}$	0.03
$Cond(D_{design}) \big/ Cond(U_{design})$	0.55

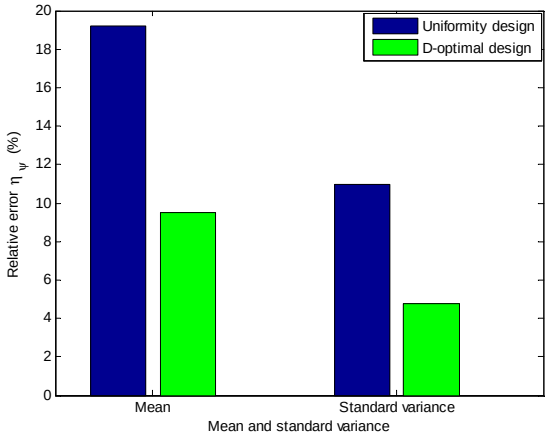

Figure 1. Mean and standard variance of η_ψ across 1000 runs

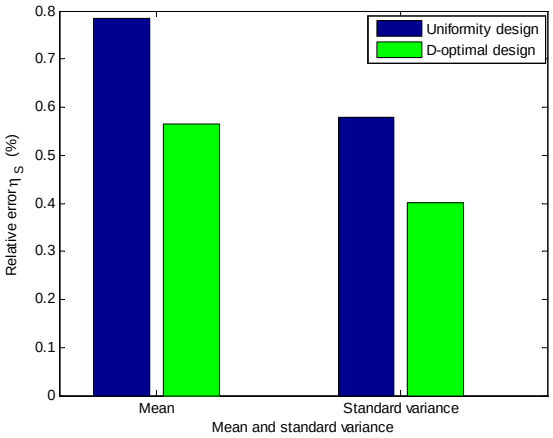

Figure 2. Mean and standard variance of η_S across 1000 runs

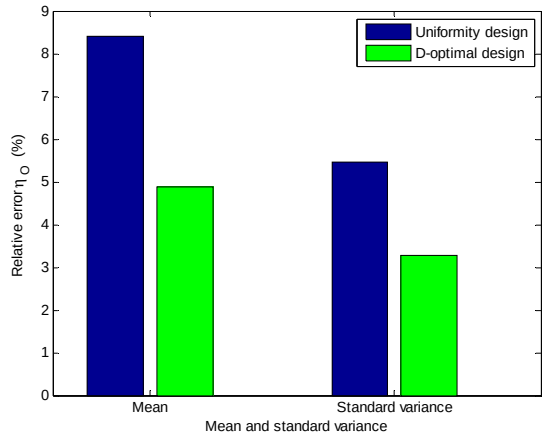

Figure 3. Mean and standard variance of η_o across 1000 runs

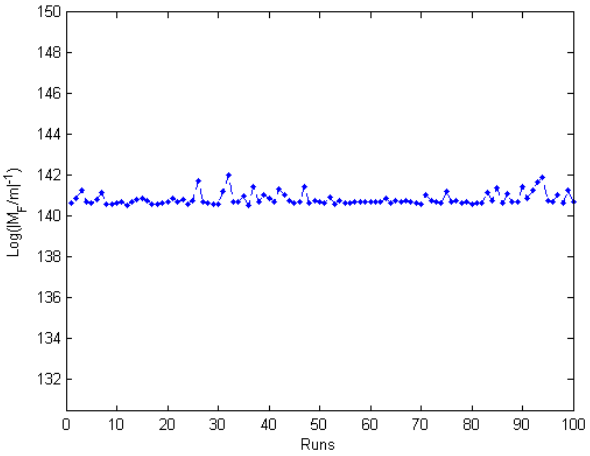

Figure 4. Final fitness values of the PSO for 100 random runs

The PSO algorithm seeks an optimal solution of the D-optimal design in a straightforward way. But this algorithm does not always to find the best solutions due to its possible premature convergence to a local optimum. Analysis of the PSO's global convergence properties has been carried out in [15]. Fig. 4 depicts the final fitness values of the cost function of the PSO across 100 random runs. It shows that all final fitness values are very close. In other words, the PSO algorithm is stable in all 100 runs. The PSO method has an ability to seek an acceptable solution without resorting to a complete search of exhaustive potential solutions.

V. CONCLUSIONS

This paper has shown that the accuracy of solutions for a magnetometer calibration problem strongly depend on the measurements distribution. We proposed to select the optimal set of the measurement positions by the D-optimal design method. The solution to D-optimal design minimum problem is obtained by a standard PSO-based algorithm. Simulation results show that the proposed method significantly improves the accuracy of the parameters estimation. The method we proposed provides maneuver guidance for the magnetometer calibration. As long as measurements on the optimal orientations are included in the collected data set for calibration, improved estimates would be achieved.

ACKNOWLEDGEMENTS

The authors thank the PhD student Jie Yang for helpful discussions.

REFERENCE

[1] Halil Ersin Soken, Chingiz Hajiyev, "UKF-Based Reconfigurable Attitude Parameters Estimation and Magnetometer Calibration," IEEE Transactions on Aerospace Electronic Systems, vol. 48, pp. 2614-2627, 2012.

[2] J. M. G. Merayo, P. Brauer, F. Primdahi, J. R. Petersen, O. V. Nielsen, "Scalar calibration of vector magnetometers," Meas. Sci. Technol., pp. 120-132, 2000.

[3] H. T. Banks, K. Holm, F. Kappel, "Comparison of optimal design methods in inverse problems," Inverse Problems, vol. 27, pp. 1-31, 2011.

[4] D. Gebre-Egziabher, G. H.Elkaim, J. D. Powell, B. W. Parkinson, "Calibration of Strapdown Magnetometers in Magnetic Field Domain," ASCE Journal of Aerospace Engineering, vol. 19, pp. 1-16, 2006.

[5] S. Bonnet, C. Bassompierre, C. Godin, S. Lesecq, A. Barraud, "Calibration methods for inertial and magnetic sensors," Sensors and Actuators A: Physical, vol. 156, pp. 302-311, 2009.

[6] P. F. de Aguiar, B. Bourguignon, M. S. Khots, D. L. Massart, R. Phan-Than-Luu, "D-optimal designs," Chemometrics and Intelligent Laboratory Systems, vol. 30, pp. 199-210, 1995.

[7] Stefan Maus, Susan Mclean, Manoj Nair, Susan Macmillan, Brian Hamilton,Alan Thomson, "The USUK World Magnetic Model for 2010-2015," 2010.

[8] C. C. Foster, G. H. Elkaim, "Extension of a Non-linear, Two-step Calibration Methodology to Include Non-Orthogonal Sensor Axes," IEEE Transactions on Aerospace Electronic Systems, vol. 44, pp. 1070-1087, 2008.

[9] Xiaofei He, "Laplacian Regularized D-Optimal Design for Active Learning and Its Application to Image Retrieval," IEEE Trans. Image Processing, vol. 19, pp. 254-263, 2010.

[10] S. Bégot, E. Voisin, P. Hiebel, E. Artioukhine, J. M. Kauffmann, "D-optimal experimental design applied to a linear magnetostatic inverse problem " IEEE Trans. Magnetics, vol. 38, pp. 1065-1068, 2002.

[11] Anne Broudiscou, Riccardo Leardi, Roger Phan-Tan-Luu, "Genetic algorithm as a tool for selection of D-optimal design," Chemometrics and Intelligent Laboratory Systems, vol. 35, pp. 105-116, 1996.

[12] James Kennedy, Russell Eberhart, "Particle Swarm Optimization," in Proceedings of the 4th IEEE International Conference on Neural Networks, Piscataway, 1995, pp. 1942-1948.

[13] Russell C. Eberhart, Yuhui Shi, "Particle swarm optimiser developments application and resources," presented at the in proceedings IEEE Congress Evolution Computation, 2001.

[14] Y. Shi, R. Eberhart, "A modified particle swarm optimizer," in Evolutionary Computation Proceedings, IEEE World Congress on Computational Intelligence, 1998, pp. 69-73.

[15] Visakan Kadirkamanathan, Kirusnapillai Selvarajah, Peter J. Fleming, "Stability Analysis of the Particle Dynamics in Particle Swarm Optimizer," IEEE Ttansactions on Evolutionary Computation, vol. 10, pp. 245-255, 2006.